JACS
JOURNAL OF THE AMERICAN CHEMICAL SOCIETY

Article

pubs.acs.org/JACS

Photoisomerization Quantum Yield of Azobenzene-Modified DNA Depends on Local Sequence

Yunqi Yan,[‡] Xin Wang,[‡] Jennifer I. L. Chen,[†] and David S. Ginger*[,‡]

[‡]Department of Chemistry, University of Washington, Seattle, Washington 98195, United States

[†]Department of Chemistry, York University, Toronto, Ontario M3J 1P3, Canada

Supporting Information

ABSTRACT: Photoswitch-modified DNA is being studied for applications including light-harvesting molecular motors, photocontrolled drug delivery, gene regulation, and optically mediated assembly of plasmonic metal nanoparticles in DNA-hybridization assays. We study the sequence and hybridization dependence of the photoisomerization quantum yield of azobenzene attached to DNA via the popular *d*-threoninol linkage. Compared to free azobenzene we find that the quantum yield for photoisomerization from trans to cis form is decreased 3-fold (from 0.094 ± 0.004 to 0.036 ± 0.002) when the azobenzene is incorporated into ssDNA, and is further reduced 15-fold (to 0.0056 ± 0.0008) for azobenzene incorporated into dsDNA. In addition, we find that the quantum yield is sensitive to the local sequence including both specific mismatches and the overall sequence-dependent melting temperature (T_m). These results serve as design rules for efficient photoswitchable DNA sequences tailored for sensing, drug delivery, and energy-harvesting applications, while also providing a foundation for understanding phenomena such as photonically controlled hybridization stringency.

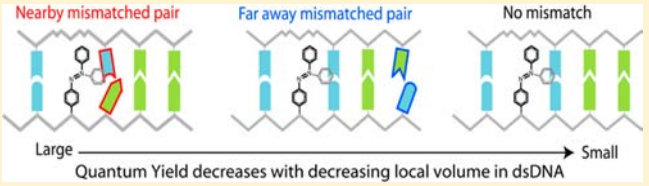

INTRODUCTION

Molecular photoswitches such as azobenzene have a long history of application in fields ranging from material science[1,2] to biology.[3] Recently, the modification of DNA with these molecules has also allowed the addition of stimulus-response functionality to a wide range of DNA-based technologies.[4−8]

Notably, Asanuma and co-workers have pioneered the development of an azobenzene-modified phosphoramidite,[9,10] which allows virtually any DNA sequences amenable to solid-phase synthesis to be readily functionalized with multiple azobenzene photoswitches. In this approach, the azobenzenes are incorporated by tethering them to additional sugar/phosphate linkages along the DNA backbone via a *d*-threoninol group (Figure 1). Despite some structural distortion of the double helix resulting from the volume of the extra phosphate and azobenzene moieties, the incorporation of a trans form azobenzene stabilizes a DNA duplex by intercalation between the neighboring bases.[11] This stabilization raises the melting temperature of the azobenzene-modified DNA above that of an otherwise identical native sequence.[12] Absorption of UV light (320−370 nm) excites the $S_0 - S_2$ transition of the azobenzene groups, promoting trans-to-cis photoisomerization. In the cis form the azobenzenes destabilize the DNA duplex, significantly lowering the melting temperature of the DNA. Blue light (~450 nm) converts the cis form back to trans, thereby permitting reversible optical control of DNA hybridization.

These developments have enabled applications ranging from photocontrolled gene regulation,[13,14] and drug delivery,[15] to optically powered molecular motors.[16,17] They have motivated proposals for DNA-based optical energy harvesting,[18] and even allowed the creation of DNA-hybridization assays capable of differentiating single-base mismatches using a photonic stringency wash.[5]

Virtually all of these applications are sensitive to the quantum yield for azobenzene photoisomerization: the total amount of optical energy required to achieve DNA denaturation and the efficiency of optically powered molecular motors will depend on the quantum yield of photoisomerization. Surprisingly, while the quantum yield for azobenzene photoisomerization is known to depend on the local environment,[19−21] there is very little data on how the quantum yield for photoisomerization of azobenzene is affected by incorporation into different DNA sequences.

Here, we address this question by studying the quantum yield of trans-to-cis photoisomerization of azobenzenes inserted into DNA sequences via the popular Asanuma chemistry.[10] We show that the quantum yield for photoisomerization decreases upon incorporation into single-stranded DNA (ssDNA), and decreases further upon incorporation into double-stranded DNA (dsDNA). Importantly, we show that the quantum yield in dsDNA is sensitive to the melting temperature of the sequence and very sensitive to the presence of local mismatches.

RESULTS AND DISCUSSION

To assess how incorporation into various DNA sequences alters the trans-to-cis photoisomerization of azobenzene we measured

Received: April 1, 2013
Published: May 10, 2013

   dx.doi.org/10.1021/ja403249u | *J. Am. Chem. Soc.* 2013, 135, 8382−8387

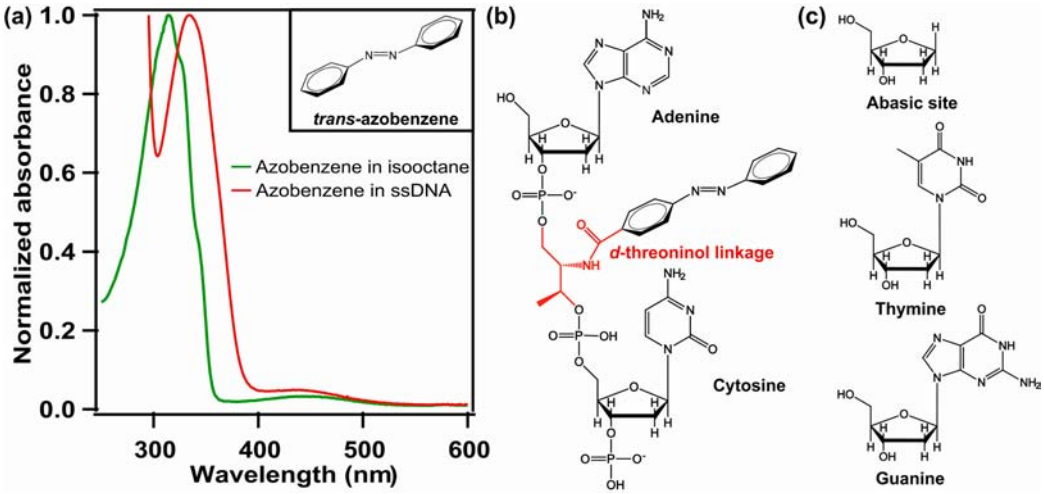

Figure 1. (a) Absorption spectra of free *trans*-azobenzene in isooctane (green) and azobenzene-modified ssDNA (red) in buffer. The structure of free azobenzene in the trans form is shown in the inset. (b) Structure of azobenzene-modified DNA with the *d*-threoninol linkage highlighted in red, and adenine and cytosine labeled. (c) DNA nucleotide structures of the abasic site, thymine, and guanine used in the sequences and described in the text.

the quantum yields in various modified DNA molecules by quantifying the fraction of *cis*-azobenzene as a function of UV (330 nm) irradiation time (Figure S2 in Supporting Information [SI]) using UV–vis absorption spectroscopy.[19,22] Figure 1a compares the absorption spectra of free *trans*-azobenzene dissolved in isooctane and *trans*-azobenzene incorporated in ssDNA in phosphate buffer. The free azobenzene exhibits the typical π-to-π^* absorption at 315 nm, whereas the azobenzene incorporated into ssDNA has its absorption band shifted to about 340 nm, as previously reported.[23]

Figure 2a compares the fraction of *cis*-azobenzene as a function of the integrated photokinetic factor[19] (excitation time converted to photon dose to account for the changing absorption of the solution over time) at 28 °C for free azobenzene, azobenzene attached via *d*-threoninol linkages[10] to a ssDNA sequence, and the same DNA sequence hybridized to its (azobenzene-free) complement. For free azobenzene, the fraction of *cis*-azobenzene at the photostationary state is 0.93, which decreases to 0.51 for azobenzene incorporated into ssDNA, and 0.15 for azobenzene incorporated into dsDNA. We extracted the photoisomerization quantum yield from the curves in Figure 2a by fitting the data to eq 1:[19,22]

$$y = (y_0 - y_\infty)\,\exp(-Ax) + y_\infty \tag{1}$$

where x is the integrated photokinetic factor[19] defined via eq 2, y is the fraction of *cis*-azobenzene (y_0 and y_∞ are the fractions of *cis*-azobenzene before photoisomerization and at the photostationary state, respectively), and A is a prefactor related to the trans-to-cis quantum yield (see SI for details). The integrated photokinetic factor is given by:

$$x(t) = \int_0^t \frac{1 - 10^{-\mathrm{abs}(t)}}{\mathrm{abs}(t)}\,\mathrm{d}t \tag{2}$$

Figure 2a shows fits of eq 1 to the data as solid lines. From these fits we obtained a quantum yield for free azobenzene of 0.094 ± 0.004 when excited at 330 nm, which is consistent with literature values.[19,22]

As can be seen from the decrease in *cis*-azobenzene fraction in the photostationary state at a given illumination intensity,

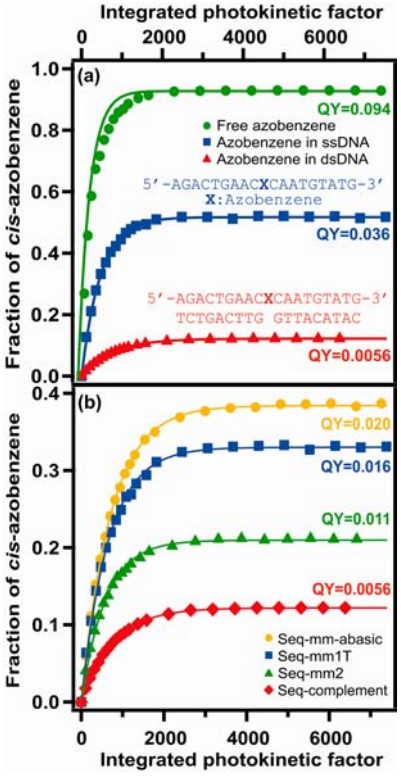

Figure 2. (a) Representative plots of the measured fraction of *cis*-azobenzene vs the integrated photokinetic factor (eq 2) used to obtain quantum yield. Solid lines are fits of eq 1 to the data shown, and are labeled with the average quantum yield values measured from at least three separate experiments. Traces are for azobenzene in isooctane (green circles), azobenzene incorporated in ssDNA (blue squares) and dsDNA (red triangles). (b) Similar plots for azobenzene incorporated in different dsDNA sequences including Seq-mm-abasic (yellow circles), Seq-mm1T (blue squares), Seq-mm2 (green triangles), and Seq-complement (red diamonds) (see Table 1 for sequences).

incorporation into the ssDNA sequence decreases the photoisomerization quantum yield by a factor of ~3 to 0.036 ± 0.002. Hybridization of the ssDNA to its complement (Seq-comple-

dx.doi.org/10.1021/ja403249u | J. Am. Chem. Soc. 2013, 135, 8382–8387

Table 1. Quantum Yields and Melting Temperatures (T_m) of the Azobenzene-Modified DNA

Names	Sequences	Quantum Yield	T_m (°C)
ssDNA	5′-AGACTGAACXCAATGTATG-3′ X: azobenzene	0.036±0.002	
Seq-mm-abasic (mm: mismatch)	5′-AGACTGAACXCAATGTATG-3′ TCTGACTTG OTTACATAC O:abasic site	0.020±0.001	46.7
Seq-mm1T	5′-AGACTGAACXCAATGTATG-3′ TCTGACTTG TTTACATAC	0.016±0.001	48.0
Seq-mm1C	5′-AGACTGAACXCAATGTATG-3′ TCTGACTTG CTTACATAC	0.015±0.001	48.0
Seq-mm1A	5′-AGACTGAACXCAATGTATG-3′ TCTGACTTG ATTACATAC	0.0078±0.0007	48.0
Seq-mm2	5′-AGACTGAACXCAATGTATG-3′ TCTGACTTG GCTACATAC	0.011±0.001	52.0
Seq-mm3	5′-AGACTGAACXCAATGTATG-3′ TCTGACTTG GTGACATAC	0.0070±0.0002	54.0
Seq-mm4	5′-AGACTGAACXCAATGTATG-3′ TCTGACTTG GTTGCATAC	0.0069±0.0006	54.0
Seq-complement	5′-AGACTGAACXCAATGTATG-3′ TCTGACTTG GTTACATAC	0.0056±0.0008	60.0

ment) results in an even more dramatic decrease of the quantum yield to 0.0056 ± 0.0008. Since the DNA solutions do not absorb at the UV excitation wavelength used here, we attribute these differences entirely to the attachment of the azobenzene to the DNA sequences.

While the structure—ssDNA or dsDNA—has a strong influence on the azobenzene photoisomerization quantum yield, we also find that the sequence of the dsDNA—particularly a mismatch in the sequence near the azobenzene site—plays a role. To explore sequence effects, we used azobenzene-modified dsDNA with one sequence having azobenzene incorporated in the center, and the other sequence bearing a single-base mismatch at varying distances from the azobenzene site (see Table 1 for sequence data). Figure 2b compares the fraction of *cis*-azobenzene as a function of the integrated photokinetic factor (eq 2) for several different dsDNA sequences at 28 °C. By fitting eq 1 to the data in Figure 2b, we extracted the photoisomerization quantum yields of the azobenzene in these different dsDNA sequences. The quantum yields for all studied sequences are summarized in Table 1. Figure 2b and the accompanying fits show that the varying fractions of *cis*-azobenzene achieved at the photostationary state are due to sequence-dependent variations in the azobenzene photoisomerization quantum yield.

Of the sequences used in Figure 2b, the lowest quantum yield of 0.0056 ± 0.0008 comes from azobenzene-modified dsDNA with no mismatches (Seq-complement). The quantum yield increases to 0.011 ± 0.001 for dsDNA having an A•C mismatch two bases away from the azobenzene position (Seq-mm2). In contrast, a C•T mismatch immediately next to the incorporated azobenzene (Seq-mm1T) increases the quantum yield by an additional 45% to 0.016 ± 0.001. Finally, we measure the largest quantum yield (0.020 ± 0.001) using modified dsDNA having an abasic site (with no purine or pyrimidine, Figure 1c, Seq-mm-abasic) as the nearest neighbor to the azobenzene in the unmodified sequence.

To examine the effects of dsDNA stability and DNA sequence on quantum yield, Figure 3 plots the quantum yield as a function of the measured melting temperature (T_m) (Figure S2 in SI) of the modified dsDNA sequences listed in Table 1. Broadly, the data show that the azobenzene quantum

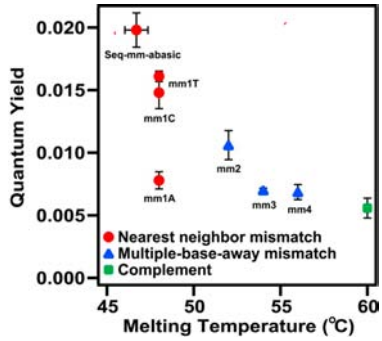

Figure 3. Trans-to-cis isomerization quantum yield plotted as a function of melting temperature (T_m) of azobenzene-modified dsDNA. Quantum yield decreases as T_m rises. The quantum yield is very sensitive to the single-base mismatch at the nearest neighbor position of the azobenzene (red circles), but is less sensitive for dsDNAs having the mismatched base multiple bases away from the azobenzene (blue triangles).

yield tends to decrease with increasing T_m of the embedding DNA sequence. We measure the highest azobenzene quantum yield (0.020 ± 0.001) for the dsDNA with the lowest T_m (46.7 °C) (Seq-mm-abasic). Likewise, we measure the lowest photoisomerization quantum yield (0.0056 ± 0.0008) for the dsDNA with the highest T_m (60.0 °C) (Seq-complement). Our data are consistent with previous work showing that photoisomerization can be used to modulate T_m,[12,24] but importantly, our work shows that the converse is also true: the T_m of the dsDNA sequence can in turn affect trans-to-cis isomerization efficiency.

Looking at these end points, one might be tempted to conclude that T_m is the primary controlling factor in determining the azobenzene quantum yield. However, closer inspection of the data reveals that more complicated effects are at work. For instance, Figure 3 shows that three sequences with very similar T_m have dramatically different quantum yields for azobenzene photoisomerization. Interestingly, all three of these sequences have a single-base mismatch immediately next to the position of the azobenzene (Seq-mm1T, Seq-mm1C, Seq-mm1A). The photoisomerization quantum yield is less sensitive to mismatches that are two or more bases away from the

dx.doi.org/10.1021/ja403249u | J. Am. Chem. Soc. 2013, 135, 8382−8387

position of the azobenzene (e.g., Seq-mm2, Seq-mm3, Seq-mm4).

We propose that the variations we observe in photoisomerization quantum yield when the azobenzene is incorporated into DNA are largely due to differences in the local free volume available to the azobenzene in the different sequences. Generally, the azobenzene quantum yield is known to depend on the free volume surrounding the azobenzene site,[20,21] and this explanation would be consistent with our results that the quantum yield decreases on going from an azobenzene free in solution to that being incorporated in ssDNA to being incorporated in dsDNA. Furthermore, this hypothesis could account for the large differences we observe between single-base mismatches that are next to the azobenzene site, and those that are further removed: distortions in the double helix are known to recover over a decay length of only a few bases.[25]

However, it is also possible that electronic interactions, including both energy and charge transfer between the azobenzene and the nucleic acid bases[11,26] are modulating the quantum yield by changing the energy relaxation pathways available to the azobenzene on an ultrafast time scale.[27] In this case, one would explain the sequence-dependent differences in quantum yield as arising from different electronic interactions between the azobenzene and the different bases. To test this alternative hypothesis, Figure 4 plots the photoisomerization quantum yield (bars) for the azobenzene incorporated in the middle of 18-base ssDNAs comprising polydeoxyadenosine (poly(dA)), polydeoxycytidine (poly(dC)), and polydeoxythymidine (poly(dT)). In comparison, Figure 4 also plots the oxidation potential of DNA nucleotides (dots) in buffer (pH = 7) as measured by Fukuzumi et al.[28] We note that, if electronic coupling were dominant, one might expect to see some correlation between oxidation potential of the neighboring bases and the quantum yield. However, Figure 4 shows that the quantum yield of azobenzene contained in poly(dA), poly(dC), and poly(dT) sequences appears uncorrelated with the oxidation potentials of the bases. On the other hand, it is known that poly(dT) is more flexible than poly(dA).[29] This result also fits well with the free volume hypothesis: azobenzene in more structurally flexible poly(dT) has a higher quantum yield than azobenzene in more rigid poly(dA). Likewise, if energy transfer were dominant, one might expect a correlation between the positions of the UV−vis spectra of the nucleotides and the measured quantum yields; however, we were unable to observe such a correlation (Figure S3 in SI). Thus, we propose that free volume is likely to be more important, while acknowledging that it will be difficult to completely separate electronic and structural control over variation in the azobenzene photoisomerization quantum yield because an increase in local free volume around the azobenzene should also tend to weaken intermolecular electronic interactions.

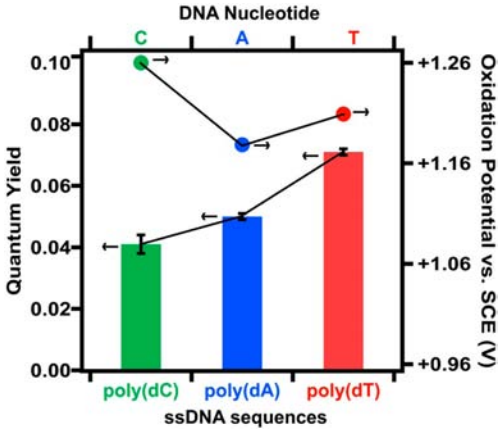

Figure 4. Quantum yield (bars) for the azobenzene incorporated into the 18-base ssDNA of poly(dC), poly(dA), and poly(dT). The oxidation potential for the individual DNA nucleotides (C, A, T) vs saturated calomel electrode (SCE) is also plotted (dots). There does not appear to be a correlation between the oxidation potential for the nucleotides and the quantum yield of the azobenzene incorporated into the ssDNA sequences as might be expected if charge transfer were the dominant factor governing azobenzene quantum yield differences between the sequences.

Finally, we can use the observed variation of azobenzene quantum yield with the DNA sequence to explain the properties of azobenzene-modified DNA that facilitate its use in novel DNA-hybridization assays.[5] Previously we have shown that using only optical inputs, DNA sequences containing single-base mismatches can be resolved in hybridization experiments involving gold nanoparticles that are heavily functionalized with azobenzene-modified DNA.[5] The resulting photonic hybridization stringency wash works because the denaturation of azobenzene-modified DNA strands occurs at lower photon doses for sequences with less complementarity. The results presented herein provide a fundamental mechanistic understanding of this process: partially mismatched sequences denature at lower photon doses because the azobenzenes in those sequences photoisomerize more efficiently than azobenzenes in perfectly complementary sequences.

To test this hypothesis, we measured the trans-to-cis isomerization quantum yield of azobenzenes incorporated in dsDNAs in a classic three-strand capture assay using a linker strand as shown in Figure 5a. The assay consists of the capture DNA modified with multiple azobenzenes (Sequence-1), the unmodified probe DNA (Sequence-2), and the unmodified target/linker (Sequence-3) that cross-hybridizes with the capture and probe sequences. We varied the target sequence by introducing a single base mismatch in the center where it will form a mismatched base pair next to the azobenzene (see sequences in Figure 5a). We measure the lowest quantum yield for the perfectly complementary sequence (Seq-perfect), and observe an increase in quantum yield from Seq-mmA, to Seq-mmC and to Seq-mmT—all having the single-base mismatch next to one of the azobenzenes. In order to compare the trend in quantum yield with that of optical hybridization stringency, we functionalized gold nanoparticles with the same capture and probe DNAs and measured the disaggregation rate of nanoparticle conjugates cross-linked by the same target DNA, which we have previously shown can exhibit photon-dose-controlled hybridization stringency.[5] We quantify the disaggregation rate by monitoring the localized surface plasmon resonance (LSPR) peak shift of nanoparticle conjugates, which is expected to blue-shift as conjugates undergo photoinduced dissociation. Indeed, the inset in Figure 5b shows that the photon-dose dependence of the nanoparticle disaggregation process follows the exact same sequence-dependent order as the measured azobenzene quantum yields, providing strong evidence that the two trends are linked.

dx.doi.org/10.1021/ja403249u | J. Am. Chem. Soc. 2013, 135, 8382−8387

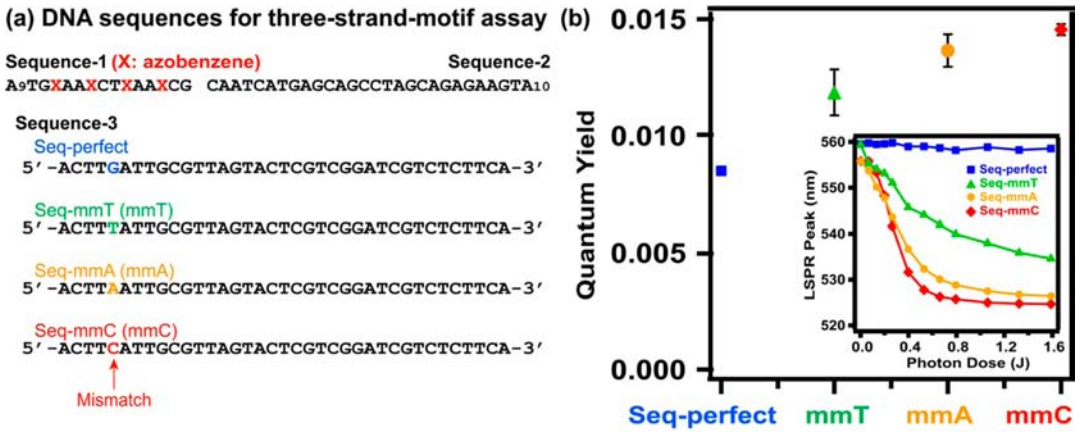

Figure 5. Trans-to-cis isomerization quantum yield explains photon-dose-controlled DNA hybridization stringency wash. (a) DNA sequences used to incorporate azobenzenes and also to cross-link gold nanoparticles. (b) The quantum yield of the azobenzene is shown against each embedding dsDNA. (Inset) Plot of the gold nanoparticle localized surface plasmon resonance (LSPR) peak position as a function of the photon dose. The azobenzene photoisomerization quantum yield increases from Seq-perfect, to Seq-mmT, to Seq-mmA and to Seq-mmC. Nanoparticle conjugates linked by these dsDNA show the same increasing order of photoinduced disaggregation rate.

CONCLUSION

We have shown that the trans-to-cis photoisomerization quantum yield for azobenzene decreases upon incorporation into DNA and is sensitive to both the local DNA sequence and DNA hybridization state. In general, the photoisomerization quantum yield tends to increase as the T_m of the attached dsDNA decreases. However, the biggest variations in quantum yield are associated with dsDNAs bearing a single-base mismatch immediately next to the azobenzene site. We propose that these variations arise due to the structural fluctuations caused by the adjacent mismatched base inducing an increase in the local free volume. Not only do these results provide a mechanism to explain optically controlled DNA hybridization stringency, but we believe they will also prove useful for designing systems to more effectively photomodulate gene regulation and drug delivery or transduce optical energy into work using DNA nanomachines.

EXPERIMENTAL METHODS

Materials. Unmodified DNAs and azobenzene-modified DNAs were purchased from Integrated DNA Technology (IDT Inc., IA). All sequences used are shown in Table 1 and Figure 5a. Water was deionized to 18.0 MΩ with the Millipore filtration system.

Preparation of dsDNA Solution. Aliquots of lyophilized DNA were dissolved in water and a desired amount of DNA aqueous solution was then brought to 0.01 M phosphate buffer (pH = 6.5), 0.1 M NaCl and 0.02% sodium azide. Equal moles of complementary DNAs were mixed at room temperature and annealed at 95 °C for 5 min. The concentration[8] of azobenzene modified dsDNA for quantum yield tests was prepared to be 10 μM; and the concentration for T_m test was 2 μM. The dsDNA solution was kept at 4 °C before use.

Preparation of the dsDNA That Has Three-Sequence Structure. The sequences for the three-strand capture assay are shown in Figure 5a. Sequence-1 and Sequence-2 are both complementary to part of Sequence-3. The annealing process consisted of two steps. First, Sequence-2 and Sequence-3 were combined and annealed at 95 °C for 5 min, followed by gradual cooling to 55 °C and holding at 55 °C for 30 min. Then, Sequence-1 was added to the solution and annealed for an additional 10 min at 55 °C. The temperature of the DNA solution was lowered to room temperature and kept at 4 °C before use.

Quantum Yield Measurements. The UV irradiation setup for quantum yield measurement consisted of an LED light source centered at 330 nm with fwhm less than 10 nm (UVTOP325HS Sensor Electronic Technology, Inc.), a homemade aluminum stage, a quartz cuvette with 1-cm optical path length, a stir plate, and a temperature controller. The temperature of the DNA solution as a function of temperature controller set point (measured in the aluminum stage) was calibrated using a thermometer. The temperature of the DNA solution was kept at 28 °C for all quantum yield measurements using the calibrated temperature controller. The UV LEDs were warmed up for 1 h, and then the illumination intensity was monitored using a silicon photodiode positioned at the other end of the aluminum stage. The UV intensity was typically 0.37−0.42 mW/cm^2. Azobenzene-modified DNA solutions were added to the quartz cuvette and were thermally equilibrated at 28 °C for 1 h in the dark before UV irradiation. During UV irradiation, UV−vis absorption spectra were recorded by an Agilent 8453 UV−vis spectrometer every 1 min for 15 min and then every 5 min for the remaining 45 min. The DNA solution was stirred during the measurement. We verified that the low intensity white light source of the spectrometer had no significant effect on the photoisomerization process (Figure S4 in SI).

Melting Temperature Measurements. An Agilent 8453 UV−vis spectrometer operating in the thermal denaturation mode was used to measure the melting temperature. The temperature ramp started at 5 °C and ended at 95 °C with 2 °C step intervals and a 5-min hold time. Melting temperature was determined as the temperature at which the first derivative of the absorbance vs temperature plot was maximum. See selected data in Figure S2 in SI.

ASSOCIATED CONTENT

Supporting Information

Plots of fraction of *cis*-azobenzene as a function of UV excitation time, melting curve of dsDNA, UV absorption coefficient spectra of DNA nucleotides, control experimental results showing UV−vis spectrometer having no interference on photoisomerization. This material is available free of charge via the Internet at http://pubs.acs.org.

AUTHOR INFORMATION

Corresponding Author

ginger@chem.washington.edu

Notes

The authors declare no competing financial interest.

ACKNOWLEDGMENTS

This paper is based on work supported by the AFOSR FA9550-10-1-0474.

REFERENCES

(1) Klajn, R. *Pure Appl. Chem.* **2010**, *82*, 2247−2279.
(2) Mahimwalla, Z.; Yager, K. G.; Mamiya, J-i.; Shishido, A.; Priimagi, A.; Barrett, C. J. *Polym. Bull.* **2012**, *69*, 967−1006.
(3) Beharry, A. A.; Woolley, G. A. *Chem. Soc. Rev.* **2011**, *40*, 4422−4437.
(4) Tanaka, F.; Mochizuki, T.; Liang, X.; Asanuma, H.; Tanaka, S.; Suzuki, K.; Kitamura, S-i.; Nishikawa, A.; Ui-Tei, K.; Hagiya, M. *Nano Lett.* **2010**, *10*, 3560−3565.
(5) Yan, Y. Q.; Chen, J. I. L.; Ginger, D. S. *Nano Lett.* **2012**, *12*, 2530−2536.
(6) Peng, L.; You, M.; Yuan, Q.; Wu, C.; Han, D.; Chen, Y.; Zhong, Z.; Xue, J.; Tan, W. *J. Am. Chem. Soc.* **2012**, *134*, 12302−12307.
(7) Yang, Y.; Endo, M.; Hidaka, K.; Sugiyama, H. *J. Am. Chem. Soc.* **2012**, *134*, 20645−20653.
(8) Nishioka, H.; Liang, X.; Kato, T.; Asanuma, H. *Angew. Chem., Int. Ed.* **2012**, *51*, 1165−1168.
(9) Asanuma, H.; Matsunaga, D.; Liu, M.; Liang, X.; Jhao, J. *Nucleic Acids Res. Suppl.* **2003**, 117−118.
(10) Asanuma, H.; Liang, X.; Nishioka, H.; Matsunaga, D.; Liu, M.; Komiyama, M. *Nat. Protoc.* **2007**, *2*, 203−212.
(11) Liang, X. G.; Asanuma, H.; Kashida, H.; Takasu, A.; Sakamoto, T.; Kawai, G.; Komiyama, M. *J. Am. Chem. Soc.* **2003**, *125*, 16408−16415.
(12) Liang, X.; Mochizuki, T.; Asanuma, H. *Small* **2009**, *5*, 1761−1768.
(13) Yamazawa, A.; Liang, X. G.; Asanuma, H.; Komiyama, M. *Angew. Chem., Int. Ed.* **2000**, *39*, 2356−2357.
(14) Matsunaga, D.; Asanuma, H.; Komiyama, M. *J. Am. Chem. Soc.* **2004**, *126*, 11452−11453.
(15) Kang, H.; Liu, H.; Zhang, X.; Yan, J.; Zhu, Z.; Peng, L.; Yang, H.; Kim, Y.; Tan, W. *Langmuir* **2011**, *27*, 399−408.
(16) Liang, X. G.; Tekenaka, N.; Nishioka, H.; Asanuma, H. *Nucleic Acids Symp. Ser.* **2008**, *52*, 697−698.
(17) Kang, H.; Liu, H.; Phillips, J. A.; Cao, Z.; Kim, Y.; Chen, Y.; Yang, Z.; Li, J.; Tan, W. *Nano Lett.* **2009**, *9*, 2690−2696.
(18) McCullagh, M.; Franco, I.; Ratner, M. A.; Schatz, G. C. *J. Am. Chem. Soc.* **2011**, *133*, 3452−3459.
(19) Rau, H. In *Photoreactive Organic Thin Films*, 1st ed.; Sekkat, Z., Kroll, W., Eds.; Elsevier: Amsterdam, 2002; pp 3−47.
(20) Mita, I.; Horie, K.; Hirao, K. *Macromolecules* **1989**, *22*, 558−563.
(21) Victor, J. G.; Torkelson, J. M. *Macromolecules* **1987**, *20*, 2241−2250.
(22) Zimmerman, G.; Chow, L. Y.; Paik, U. J. *J. Am. Chem. Soc.* **1958**, *80*, 3528−3531.
(23) Asanuma, H.; Ito, T.; Komiyama, M. *Tetrahedron Lett.* **1998**, *39*, 9015−9018.
(24) Kamei, T.; Akiyama, H.; Morii, H.; Tamaoki, N.; Uyeda, T. Q. P. *Nucleosides, Nucleotides Nucleic Acids* **2011**, *28*, 12−28.
(25) McCullagh, M.; Franco, I.; Ratner, M. A.; Schatz, G. C. *J. Phys. Chem. Lett.* **2012**, *3*, 689−693.
(26) Lewis, F. D.; Wu, Y. S.; Zhang, L. G.; Zuo, X. B.; Hayes, R. T.; Wasielewski, M. R. *J. Am. Chem. Soc.* **2004**, *126*, 8206−8215.
(27) Chen, T.; Igarashi, K.; Nakagawa, N.; Yamane, K.; Fujii, T.; Asanuma, H.; Yamashita, M. *J. Photochem. Photobiol., A* **2011**, *223*, 119−123.
(28) Fukuzumi, S.; Miyao, H.; Ohkubo, K.; Suenobu, T. *J. Phys. Chem. A* **2005**, *109*, 3285−3294.
(29) Goddard, N. L.; Bonnet, G.; Krichevsky, O.; Libchaber, A. *Phys. Rev. Lett.* **2000**, *85*, 2400−2403.